Vanadium surface oxides on Pd(111): A structural analysis

C. Klein,[1] G. Kresse,[2] S. Surnev,[3] F. P. Netzer,[3] M. Schmid,[1] and P. Varga[1]
[1]*Institut für Allgemeine Physik, Vienna University of Technology, A-1040 Vienna, Austria*
[2]*Institut für Materialphysik and CMS, University of Vienna, A-1090 Vienna, Austria*
[3]*Institut für Experimentalphysik, Karl-Franzens-Universität Graz, A-8010 Graz, Austria*
(Received 13 August 2003; published 30 December 2003)

Scanning tunneling microscopy studies of vanadium oxides grown on Pd(111) show interesting structures especially in the low-coverage region. Evaporation of V in an oxygen background at elevated sample temperature (250 °C) results in the formation of a nonperiodic honeycomb-like structure growing from the steps, which starts to transform into an ordered phase at a vanadium coverage of ≈0.2 ML (monolayer). At 0.31 ML the entire surface is covered by this well-ordered open (4×4) structure. Annealing this structure in H_2 atmosphere transforms the phase into a V_2O_3 surface oxide with (2×2) periodicity, whose optimal coverage is reached at 0.5 ML vanadium. Models for both ordered structures have been suggested before on the basis of *ab initio* density-functional theory (DFT) calculations and molecular-dynamics simulations and these models are now unambiguously confirmed by quantitative low-energy electron-diffraction (LEED) analyses. In the (4×4) phase, the V atoms are surrounded by four oxygen atoms in an unusual tetrahedral coordination leading to a V_5O_{14} stoichiometry. This tetrahedral coordination allows the oxide to adopt open loosely packed two-dimensional (2D) and 1D structures, which are stabilized by the surface-oxide interface energy. Furthermore, it is shown that state of the art DFT calculations can indeed predict complex structures exactly as well as that modern quantitative LEED is capable of dealing with very large unit cells.

DOI: 10.1103/PhysRevB.68.235416 PACS number(s): 68.47.Gh, 68.37.Ef, 61.14.Hg, 68.43.Bc

I. INTRODUCTION

Vanadium oxides play an important role in many technological applications (e.g., batteries, sensors) and especially in catalysis.[1,2] Because of the wide range of oxidation states of vanadium [VO (V^{2+}), V_2O_3 (V^{3+}), VO_2(V^{4+}), and V_2O_5 (V^{5+})], vanadium oxides can serve as catalysts in oxidation as well as reduction reactions. In this respect, mainly vanadium oxides supported on TiO_2 have been a very active field of research due to their excellent catalytic abilities. Generally speaking, it has been found that the catalytic activity of certain ultrathin vanadia films is increased in a profound way compared to bulk oxides.[3] This support mediated effect, however, is still not completely understood. One reason for that is the lack of knowledge about the structural details of those oxides. Since vanadia layers tend to form many different surface structures simultaneously, a conventional structure analysis using diffraction techniques such as low-energy electron diffraction (LEED) or surface x-ray diffraction is quite difficult. Nevertheless, those mixed phases can be depicted using local probe techniques such as scanning tunneling microscopy (STM).[4] One finding is that whenever a vanadium oxide is grown on a support, the established phase depends strongly on the deposition conditions.[5] In the present work it is shown that a careful preparation under appropriate conditions enables the growth of well-ordered two-dimensional vanadium oxides on Pd(111) covering the entire surface, making a quantitative LEED analysis possible.

Although the growth of thin vanadium oxide films on Pd(111) has been intensely investigated by STM and density-functional theory (DFT),[4,6–8] the structures formed in the oxygen rich regime with a vanadium coverage below 0.3 ML [monolayers; 1 ML equals the number of Pd atoms in a Pd(111) plane] have not been analyzed in detail so far. In this paper, we present results on this low vanadium coverage range, showing the formation of a nonperiodic vanadium oxide at 0.1 ML, which already incorporates building blocks of the well-ordered (4×4) phase. The latter structure starts to form at 0.2 ML coverage. A STM study of the transformation from the unordered, nonperiodic oxide structure to the above mentioned (4×4) structure, which finally covers the whole surface at 0.31 ML, is presented. The (4×4) phase is identical to the one reported in Refs. 4, 9, and 10, which was found to be very unstable due to its easy reduction by hydrogen. We therefore include a short paragraph dealing with the structural changes caused by this reduction process, covering the description of the necessary steps for a complete transformation of the (4×4) to a (2×2) phase. However, the main focus of this work lies on the structural analysis of the highly ordered (2×2) and (4×4) phases including a detailed DFT and quantitative LEED analysis. Models for both structures have been suggested before, but, in particular, the (4×4) phase is so unusual that further experimental support for the uncommon tetrahedral coordination of the vanadium atoms is required. This unambiguous support is provided here by a careful LEED analysis.

II. EXPERIMENT AND CALCULATION

The experiments were carried out in Vienna in two different ultrahigh vacuum chambers with base pressures in the low 10^{-11}-mbar range. The hydrogen partial pressure, in particular, was below 10^{-11} mbar, preventing an unintended reduction of the prepared oxides. Prior to all STM measurements an additional chamber was used for sample preparation with a base pressure also below 10^{-10} mbar. Both analysis chambers were equipped with a quadrupole

 ©2003 The American Physical Society

mass spectrometer which gave detailed information on the composition of the residual gas, making sure that the residual gas pressure was sufficiently low, especially with respect to hydrogen. The STM measurements were done at room temperature using a customized Omicron micro-STM with an electrochemically etched tungsten tip, which was cleaned in the preparation chamber by Ar^+ bombardment. All STM images presented in this study were taken in the constant current mode.

The LEED measurements were performed at normal incidence of the primary electron beam using a two-grid system and video data acquisition. The LEED patterns were stored as 8-bit images and subsequently analyzed by an image processing program which extracted the *I-V* spectra for each visible beam. For improvement of the quality of the LEED images, an image processing sequence similar to the one used for astronomical charge-coupled device (CCD) images was implemented (cf. Ref. 11) prior to the evalulation of the spot intensities. After background subtraction and normalization to the emitted electron current, the *I-V* spectra were averaged over symmetry-equivalent beams and smoothed in the Fourier domain. Finally, to maximize the quality of the spectra, the results of several equivalent measurements were averaged.

The LEED calculations were done using the TENSERLEED program package,[12] where the Tensor-LEED perturbation method is implemented, facilitating the search for the correct structure considerably, especially if the parameter space is rather large. For the large supercells presented in this study a parallelization of the full dynamical calculations was necessary, which was realized by splitting the energy range into small pieces that were reassembled afterwards. To determine the agreement between measured and calculated *I-V* curves the Pendry *R* factor[13] was chosen. The error bars given in this paper were derived from Pendry's variance, namely by varying a certain parameter away from the best-fit structure until the difference between the according *R* factor and the best-fit value got larger than this variance. To reduce the computational effort, all other parameters were fixed to the best-fit structure, so no subsequent reoptimization was performed, thus the error bars do not account for coupling between search parameters.

The *ab initio* calculations were performed using the Vienna *ab initio* simulation package (VASP).[14] The interaction between the electrons and ions was described by the projector augmented wave method in the implementation of Kresse and Joubert.[15] The precise calculational setup was already described in a number of papers and is therefore not repeated here. For details we refer in particular to Ref. 10, where more information on the calculation of the (4×4) structures is given, and to Ref. 8 for the general construction of *ab initio* phase diagrams for oxides on a metal support.

III. SAMPLE PREPARATION

To prepare a clean Pd(111) surface the crystal was sputtered by 2-keV Ar^+ ions at room temperature and 600 °C, followed by an annealing step at 800 °C. In all cases, electron bombardment from the back side was used as heating mechanism. Additionally, the crystal was exposed to molecular oxygen (2×10^{-7} mbar) at 600 °C, cooled down to 100 °C in oxygen atmosphere, followed by a flash to 800 °C to get rid of disturbing impurities. The cleanliness of the sample was then checked by Auger electron spectroscopy and LEED, showing no contaminations. The oxygen treatment, however, was performed as an initial sample-cleaning step only and found to be unnecessary for later oxide preparations.

The vanadium oxide was prepared following the procedures described in Ref. 4, namely by evaporating V from a water-cooled electron-beam evaporator. Additionally, a retarding voltage was applied to the end of the evaporator in order to prevent unintentional sputtering of the crystal by high-energy V ions. V was deposited on the heated Pd(111) crystal (250 °C) in oxygen atmosphere ($p_{O_2}=2\times10^{-7}$ mbar) at a deposition rate of $\approx$0.25 ML/min. The amount of deposited V was determined by a quartz-crystal microbalance and was varied between 0.1 and 0.3 ML. After deposition the sample was cooled down in oxygen atmosphere to prevent unintentional reduction of the vanadium-oxide layer.

In the following, whenever we refer to a certain coverage, the value given represents the V coverage in units of V atoms per Pd(111) surface unit cell.

IV. RESULTS AND DISCUSSION

A. STM

Figure 1(a) shows a STM image of the Pd(111) crystal after deposition of 0.1 ML vanadium in oxygen atmosphere as described above. Already at this low coverage a nonperiodic honeycomb-like oxide starts to grow from the steps. The Auger peak-to-peak height of the V peak at 477 eV corresponding to this coverage was measured to be 1.5% of the main Pd peak at 330 eV. In the case of large terraces (width $>$500 Å) also the formation of islands was observed. With a maximum diameter of about 22.1 Å, the size of these hexagons can be very large and it varies considerably, depending on the vanadium coverage. For comparison, the nearest-neighbor distance on a Pd(111) surface is 2.75 Å, which means that the biggest hexagons are comparable in size to an (8×8) supercell.

At a certain amount of deposited vanadium ($\approx$0.15 ML) nearly the entire surface is covered by this nonperiodic phase. From this coverage on, a partial transformation from the original nonperiodic phase to a quasiordered phase starts to occur, which consists of a characteristic, nearly periodic arrangement of large hexagons being surrounded by six small ones [bottom right in Fig. 1(b)]. The corresponding supercell size would be (11×11) [cf. white rhomb in Fig. 1(b)]. However, the size of these hexagons varies too much for superstructure spots to be observable by LEED. The apparent height of the hexagon sides with respect to the Pd(111) surface was measured to be 1.3 Å and the corrugation amplitude between maxima and minima within the honeycomb-like structure was 0.9 Å.

Further increase of the vanadium coverage results in a decrease of the average honeycomb size, eventually leading

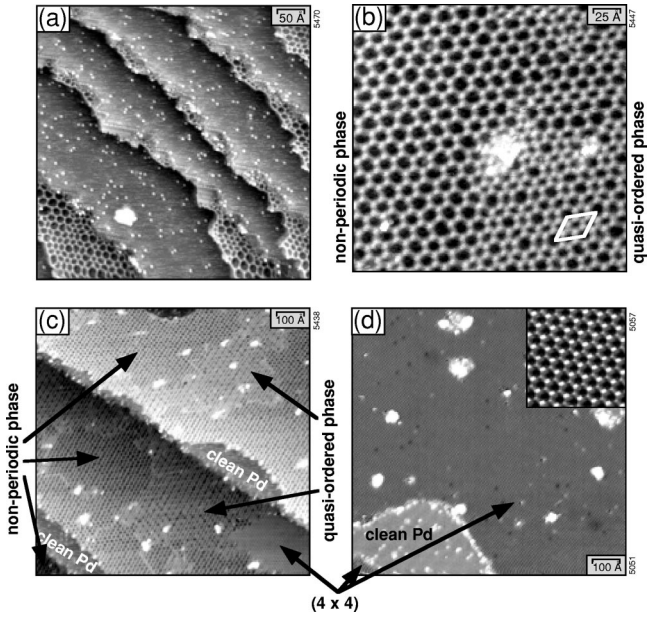

FIG. 1. Room-temperature STM images of vanadium oxides grown on Pd(111) at different vanadium coverages. (a) Image of a nonperiodic oxide beginning to grow from the steps (500×500 Å^2, -1.03 V, 0.46 nA, 0.1 ML). (b) High-resolution image of coexisting quasi-ordered and nonperiodic phases (250×240 Å^2, -1.05 V, 0.46 nA, 0.2 ML). (c) Large scale image obtained after deposition of 0.2-ML vanadium, showing a coexistence of three different oxide phases (1000×1000 Å^2, -1.09 V, 0.46 nA, 0.2 ML). (d) Large scale image of the (4×4) phase, covering almost the entire surface (1000×1000 Å^2, -0.10 V, 0.46 nA, 0.3 ML); the inset in the upper right corner shows an atomically resolved magnification of a (4×4) area (71×69 Å^2, -0.05 V, 0.46 nA).

to the formation of an ordered (4×4) structure starting at ≈0.2 ML [Fig. 1(c)]. In this STM image one can identify all three different vanadium oxide phases at once, i.e., the nonperiodic, the quasiordered, and a rather small area covered with the above-mentioned, ordered (4×4) structure. This ordering can already be observed by LEED, showing a weak (4×4) diffraction pattern. Increasing the vanadium-oxide coverage above 0.2 ML causes the surface area covered by the (4×4) structure to grow at the expense of the low-coverage phases. At the optimal coverage of ≈0.3 ML this perfectly ordered phase covers the entire surface [Fig. 1(d)], resulting in a very sharp LEED pattern. The corresponding vanadium Auger peak-to-peak height was found to be $\approx4.5\%$. Increasing the coverage above this ideal value results in the formation of other structures as observed in Ref. 7. Compared to the low coverage phases, the (4×4) structure seems higher by 0.7 Å, which amounts to an apparent height of 2.0 Å above Pd(111). Also the observed corrugation of 1.1 Å is similar to the one mentioned in Ref. 4.

The (4×4) structure, however, is easily reduced in the presence of hydrogen.[8] Upon hydrogen exposure the (4×4) structure begins to dissolve, starting at the phase boundaries to the low-coverage phases. Figure 2 shows STM images of the decomposition of the above described phases in a hydrogen background pressure of 4×10^{-9} mbar. Already after dosing 0.24 L (1 Langmuir$=10^{-6}$ torr s; hydrogen doses given in this paper are corrected for the sensitivity of the ion gauge) of molecular hydrogen, part of the low-coverage phases starts to disintegrate [Fig. 2(b)], whereas the (4×4) structure remains predominantly stable until an overall hydrogen dose of ≈1 L, which is reached at the end of Fig. 2(c). After the exposure to 2.1 L all former phases are completely decomposed, resulting in a network of branches with a local (2×2) symmetry [Fig. 2(f)]. Heating the crystal up to 300 °C (5 min) smoothens the surface, resulting in large (2×2) regions, separated by clean Pd(111) areas. We want to stress the fact that complete reduction by H_2 always results exclusively in those (2×2) areas, removing all other phases, up to a vanadium coverage of 0.5 ML. These (2×2) domains are structurally equal to the (2×2) phase described in Ref. 7, indicating this structure to be the most stable one at lower chemical potential of oxygen and a vanadium coverage below 0.5 ML.

B. (2×2) structure

1. Preparation of the (2×2) structure for LEED

After sputtering and annealing of the crystal, 0.3 ML of vanadium were deposited in an oxygen background as described previously. To obtain a pure (2×2) reconstruction the sample had to undergo a hydrogen treatment at 250 °C and 1×10^{-7} mbar hydrogen partial pressure for 5 min, resulting in very sharp (2×2) superstructure spots. Since this preparation results in a vanadium oxide surface coverage of $\approx60\%$, one is always confronted with a coexistence of the well-ordered (2×2) phase together with clean Pd(111) areas, which has to be taken into account in the quantitative LEED calculations.

2. LEED analysis

For the LEED *I-V* analysis LEED patterns starting from 30 eV up to 350 eV, with a step width of 1 eV, were recorded. This enabled the extraction of 12 symmetry-inequivalent beam sets (five integer and seven fractional order beams) and resulted in a cumulative energy range of 2120 eV. The structural models treated in the quantitative LEED analysis of this surface oxide are similar to the ones proposed in Ref. 4 and are shown in Fig. 3. For optimization, the first four Pd interlayer distances and the vanadium and oxygen vertical coordinates were varied within the Tensor-LEED framework. Additionally, buckling and pairing of the surface oxide and the first Pd layer were considered, as well as a variation of the vibrational amplitudes of these atoms. The imaginary part of the inner potential was optimized full-dynamically, both (the real and imaginary) parts were kept energy independent. Furthermore, the vibrational amplitudes of the Pd bulk were allowed to vary slightly for the determination of the best-fit structure. The result of this structural LEED analysis is a confirmation of the model originally proposed by DFT,[7] favoring a surface oxide with V_2O_3 stoichiometry (cf. Fig. 3). Assuming a surface fully covered with the (2×2) structure, a Pendry *R* factor of 0.23 is already achieved, with a considerably higher *R* factor of the integer

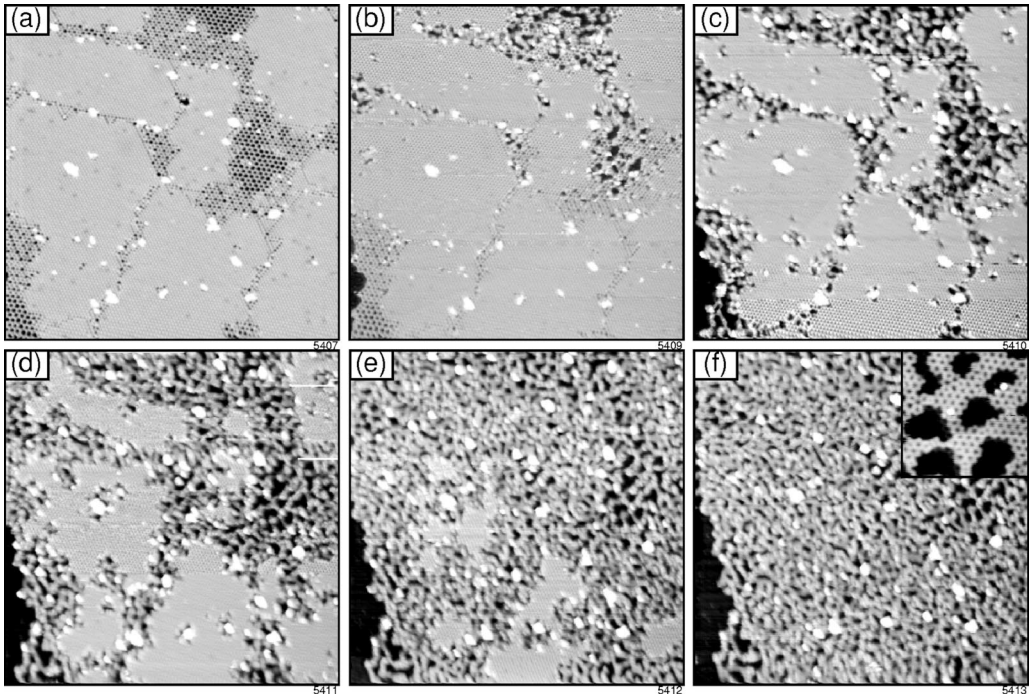

FIG. 2. STM images of the same area of a Pd(111) crystal covered with 0.3 ML vanadium oxide (1000×1000 Å^2, -1.1 V, 0.46 nA). (a) Surface structure before the exposure to hydrogen showing large well-ordered (4×4) areas separated by rather small regions composed of the low-coverage phases. (b)–(f) Images taken at a hydrogen background pressure of 4×10^{-9} mbar, the time difference between two successive images was 2.2 min, which is equivalent to a hydrogen dose of 0.53 L. During the reduction process all former phases are completely decomposed resulting in a network of branches with local (2×2) symmetry [cf. inset of (f) (81×82 Å^2, -1.07 V, 0.46 nA)].

beams ($R_{\mathrm{Pe}}^{\mathrm{int}}=0.27$) as compared to the superstructure (fractional) beams ($R_{\mathrm{Pe}}^{\mathrm{frac}}=0.20$). This rather high value of the R factor for the integer order beams is caused by the disregard of the clean Pd(111) areas. We have therefore taken the coexistence of clean Pd(111) surface areas into account by domain mixing in the LEED calculations, i.e., the I-V curves of an unreconstructed, clean Pd(111) surface were averaged with the I-V curves of the surface oxide. For the structural search the first interlayer distance of the clean Pd(111) domains and its surface vibration amplitude were free parameters, whereas the interlayer distances of the deeper layers were assumed to be the same for the clean Pd(111) and the oxide domains, in order to reduce the number of free parameters. In the final structural search 12 parameters were independently varied, which resulted in a V_2O_3 surface coverage of 70% and an overall R factor of 0.16. The agreement is indeed excellent, especially considering the problems of LEED in dealing with open structures (cf., e.g., Ref. 16). Moreover, the agreement with the DFT values is very reasonable (cf. Table I), the only obvious difference being the buckling of the first Pd layer, which might stem from the disregard of the space dependence of the inner potential caused by the atomic roughness of the surface oxide. In order to allow a direct comparison between theory and experiment, the theoretical positions were scaled by the ratio of the theoretical and experimental Pd lattice constant $a_{\mathrm{theory}}/a_{\mathrm{exp}}=1.016$ (experimental in-plane nearest-neighbor distance 2.7506 Å, experimental bulk interlayer distance 2.246 Å). The optimized vibrational amplitudes are also given in Table I, all others were fixed to the bulk value of 0.12 Å. The best-fit values of the inner potential were $V_{0r}=7$ eV and $V_{0i}=5$ eV, respectively. Finally, although horizontal displacements (pairing) of the oxygen atoms and the Pd atoms in the first layer were considered, this kind of reconstruction was not found to occur for this structure. Consequently, the O atoms reside exactly above the 1st-layer V atoms. In other words, the V_2O_3 overlayer forms a honeycomb structure with sixfold rotational symmetry. At first glance, this vanadium oxide bears some resemblance to the (4×4) silver oxide on Ag(111) phase, where a similar honeycomb-like structure was observed, though with the oxygen atoms (not the metal) at the corners of the hexagons.[17,18] As a result, in the silver oxide the Ag atoms have two oxygen neighbors, in contrast to three O atoms neighboring the vanadium atoms in the present structure. We attribute this difference to the different oxidation states of V^{3+} and Ag^{1+}, which are responsible for the exchanged atomic positions of metal and oxygen. All in all, the successful determination of the structural parameters of the (2×2) structure showed the applicability of quantitative LEED to this kind of vanadium surface oxides and encouraged the analysis of the far more complicated (4×4) structure.

C. (4×4) structure

As described above, without any further treatment deposition of 0.3 ML vanadium in O_2 atmosphere results in the formation of a perfectly ordered structure with a (4×4) pe-

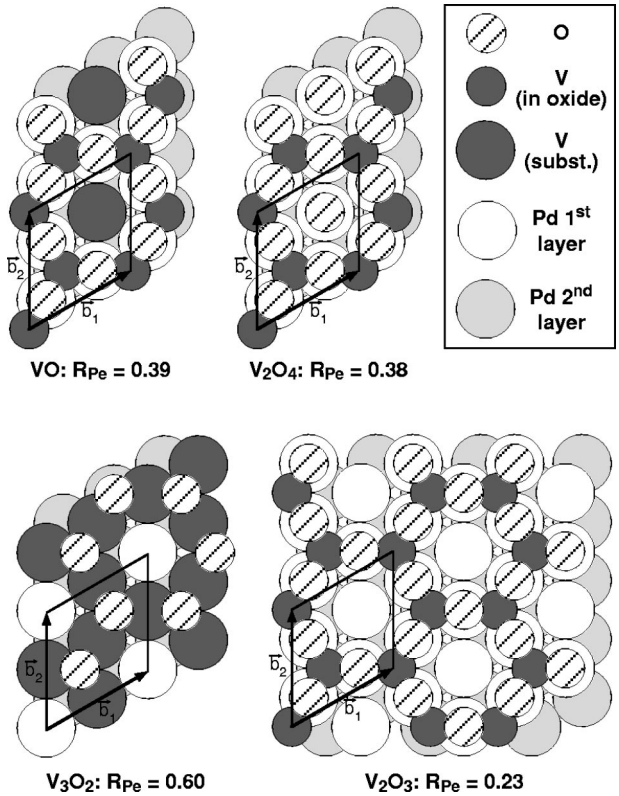

FIG. 3. Structural models for the (2×2) superstructure considered in the quantitative LEED analysis. Hatched spheres represent oxygen atoms, whereas dark-gray spheres are vanadium atoms—the rest are palladium atoms of the first and the second substrate layer. Pendry R factors shown do not account for the coexistence of clean Pd(111) (see text).

riodicity. The quality of the oxide strongly depends on the amount of deposited vanadium (0.31 ML for a perfect layer, see below) as well as on the quality of the vacuum. This surface oxide was found to be stable at room temperature as long as the hydrogen exposure remained well below 1 L.

1. DFT calculations

The determination of a reasonable structural model for the (4×4) phase was based on extensive *ab initio* modeling making use of finite temperature molecular dynamics.[19] The initial *ab initio* calculations were carried out using rather thin three-layer-thick Pd slabs and a single off-symmetry k-point with the coordinates (0.25, 0.25, 0.0). Such a setup allows for a fairly rapid screening of many conceivable structural models. The information available from experiment is unfortunately rather limited. One crucial hint, however, is that the reduction of the (4×4) phase covering the entire surface leads to the (2×2) surface-V_2O_3 structure with the oxide covering 60%–70% of the total surface area.[10] This allows to determine the number of vanadium atoms in the (4×4) cell to be either six or five. Furthermore, the measured core levels suggest that the ratio between oxygen and vanadium atoms should be close to 5:2, similar to the bulk V_2O_5 phase.[4] The only other information available was the honeycomb-like image observed in STM.

TABLE I. Comparison between the LEED and *ab initio* results for the (2×2) surface-V_2O_3 structural parameters. Here, d_{xy} denotes the averaged vertical distance between atoms/layer x and atoms/layer y; b_{Pd1} represents the buckling of the topmost Pd layer (with the "freestanding" Pd center atom up).

Parameters	LEED (Pure V_2O_3)	LEED (Domain mixing)	VASP
$\mathrm{vib_O}$ (Å)	0.32	0.27 ± 0.08	
d_{OV} (Å)	0.66	0.68 ± 0.08	0.71
$\mathrm{vib_V}$ (Å)	0.20	0.18 ± 0.04	
d_{VPd1} (Å)	2.10	2.10 ± 0.03	2.11
b_{Pd1} (Å)	0.08	0.10 ± 0.04	-0.04
$\mathrm{vib_{Pd_{center}}}$ (Å)	0.15	0.14 ± 0.05	
$\mathrm{vib_{Pd1}}$ (Å)	0.13	0.13 ± 0.05	
$\Delta d_{12}(\%)$	$+0.62$	$+0.66\pm1.2$	$+1.96$
$\Delta d_{23}(\%)$	$+1.07$	$+0.00\pm1.87$	$+0.18$
$\Delta d_{34}(\%)$	-1.16	-0.89 ± 1.91	$+0$
d_{bulk}	2.246	2.246	2.246
R_{Pe}	0.23	0.16	

Screening of possible structural models started from models inspired by the surface-V_2O_3 structure, albeit, with a less dense packing and an appropriate number of oxygen atoms coordinated only to a single V instead of two V atoms. This increases the oxygen content of the structure compared to the surface-V_2O_3 phase. The stringent requirement for a reasonable candidate is that it should be stable in the surface phase diagrams constructed according to the prescription of Ref. 8. To meet this criterion the formation energy of the surface oxide must be larger than that of bulk V_2O_5. However, none of the initially considered structures fulfilled this criterion, on the contrary, they were generally rather unfavorable.

In the next step, an attempt was made to interlink octahedral VO_6 building units in such a way that a honeycomb-like structure is generated. This attempt however failed already at the stage of constructing appropriate models and led to the important conclusion that it is not possible to generate "open-pored" two-dimensional (2D) thin oxide films, if the octahedral V coordination is maintained. The octahedral coordination allows only for densely packed 2D or 3D oxides. One-dimensional chain-like such as units, which are required for a loose packing, cannot be assembled using octahedrons, at least not for reasonable oxidation states of vanadium. Partly this is also observed in the bulk oxides, where the less densely packed V_2O_5 structure exhibits a pyramidal instead of octahedral coordination.

To explain the observed structures, a different strategy is required, and a tetrahedral coordination of the V atoms in the oxide is one intriguing possibility. Tetrahedral VO_4 units can be interlinked much more readily in a manner that allows to form open 2D structures and 1D chains. But it is certain that the tetrahedral coordination is less favorable than the octahedral one for vanadium oxides. The larger interaction energy of the open oxide structure with the surface must make up for this energy penalty. Several structures were constructed by interlinking tetrahedra, and the calculated energies were indeed found to be rather close to those of V_2O_5, but yet not

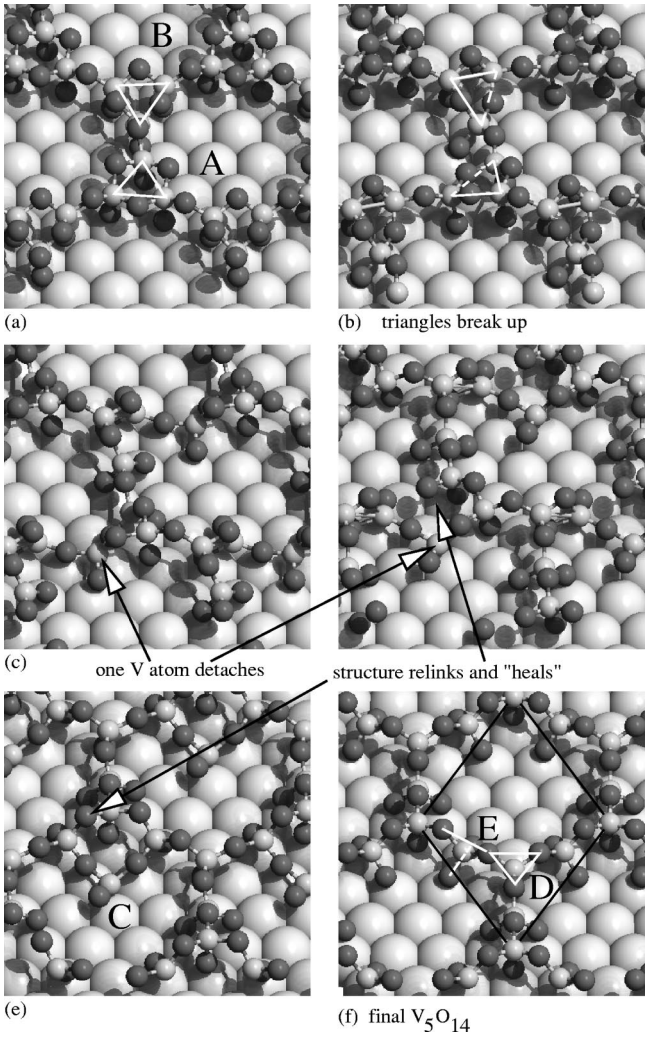

FIG. 4. Snapshots of the finite temperature molecular-dynamics simulation of a V_6O_{15} surface oxide in a (4×4) Pd(111) surface cell. Images were taken every 0.4 ps. The final image shows the optimized V_5O_{14} geometry as determined by DFT. Small light-gray and dark-gray balls are the vanadium and oxygen atoms, respectively. The black lines in (f) indicate the unit cell of the final (4×4)-V_5O_{14} structure.

stable enough to compete with other previously determined structures at the surface.[8] In addition, none of the new structures exhibited agreement with the observed STM image. In a final attempt, the most stable candidate was subjected to a simple finite temperature *ab initio* molecular-dynamics (MD) simulation, in which the temperature was initially set to 1500 K and then gradually decreased to 500 K. Since the model contains around 60 atoms, the simulation time had to be kept short, to a total of 5000 time steps with a time step of 1 fs. Snapshots of this simulation are shown in Fig. 4. For the initial configuration six tetrahedral units per (4×4) surface cell are visible (V_6O_{15}). Three of these units are interlinked to form a triangle (marked *A*) and the three remaining units are connected to form an inverted triangle (marked *B*). The triangles *A* and *B* are linked in such a manner that a honeycomb-like pattern is created. All together a reasonable structural guess, but, as already mentioned, the structure is neither sufficiently stable nor does it reproduce the experimental STM image (each triangle would be visualized as a triangle in the STM). The MD simulation leads to a rapid change of the structure. After 0.4 ps, both triangles start to break up (second and third snapshots), then one of the V atoms detaches from the oxide and binds directly to the substrate (third and forth snapshots), and finally the structure heals to form again a tetrahedrally coordinated network, with five tetrahedral units.

This structure is not yet stable in the phase diagram, but it contains a VO unit (Fig. 4, *C*), which reduces the otherwise high symmetry. When this single unit is removed the final structural model with the stoichiometry V_5O_{14} is obtained. It has all the desired properties, i.e., its formation energy is sufficiently large that the structure shows up in the surface phase diagram (compare Ref. 10), the simulated STM images agree very well with the observed images (see below), and the calculated vibrational frequencies match rather well to those measured by high-resolution electron energy-loss spectroscopy.[10] The final structure has in fact rather remarkable properties. It is characterized by VO_4 tetrahedrons, which are interlinked in two different manners. Either the trigonal base of the tetrahedron is parallel to the surface plane with the tip of the tetrahedron pointing towards the substrate (Fig. 4, *D*), or two edges of the tetrahedron are parallel to the surface plane (Fig. 4, *E*). In the latter case,

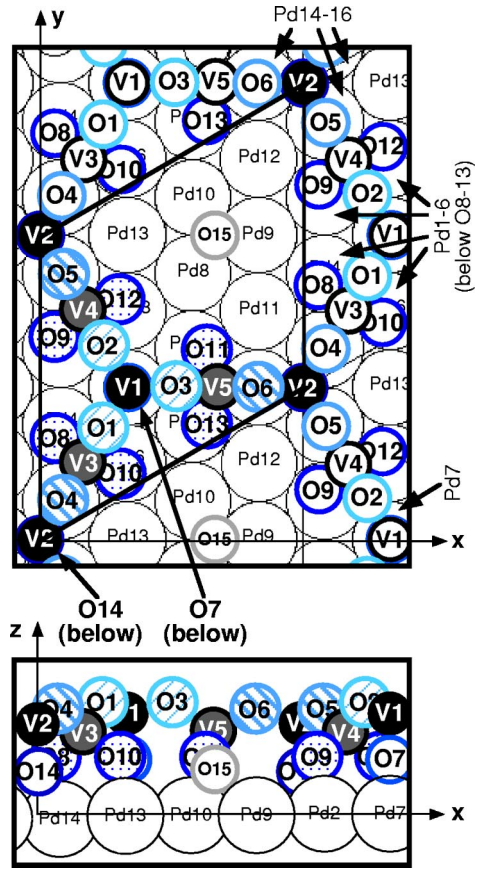

FIG. 5. (Color online) Top and side views of the structure model for the (4×4)-V_5O_{14} surface oxide on Pd(111), consisting of 19 oxide atoms per supercell. Due to the high symmetry of the structure only eight oxide atoms can be independently varied.

two O atoms are located on top of Pd atoms, binding the oxide to the substrate. The adsorption energy of this oxide on the surface, which is defined as the energy gain for bringing the oxide from the vacuum to the surface, is 10 eV per (4×4) surface cell. Since eight oxygen atoms are coordinated to the surface, an interaction energy of 1.25 eV is calculated per oxygen atom in contact with the surface, which is notably larger than for other oxides.[8] Additionally the structure allows for a relatively large fraction of the oxygen atoms to be coordinated to the substrate (8 out of 14). Both factors are decisive for the stability of the surface oxide. We also note that the oxide is overstoichiometric, i.e., $14/5>5/2$; it contains more oxygen atoms than any known bulk vanadium oxide. This is only possible because the substrate transfers charge to the oxygen atoms.

Additionally, it is very likely that a single oxygen atom is located in the otherwise empty center of this oxide structure (atom O15 in Fig. 5), indicated by a theoretical adsorption energy of -1.2 eV, which is only 0.16 eV lower than the value for the chemisorbed O-(2×2) superstructure $(-1.36$ eV).

2. LEED analysis

For the LEED analysis of the (4×4) structure the electron energy was varied between 30 and 300 eV and 15 independent beam sets were analyzed. The useful data extracted from five integer and ten fractional order beam sets amounted to a total energy range of 2300 eV. Starting from the oxide structure found by the *ab initio* calculation, two different types of stacking were investigated, favoring, after a first optimization step, the one proposed by DFT ($R_{\mathrm{Pe}}=0.45$ vs $R_{\mathrm{Pe}}=0.62$, for the V2 atoms of Fig. 5 being located in hcp vs fcc sites, respectively). Due to the high symmetry of the V_5O_{14} structure only 8 out of 19 oxide atoms can be independently varied (cf. Fig. 5), thus reducing the number of parameters considerably, which therefore increases the reliability of the LEED analysis for this extremely complex structure.

By optimizing the vertical coordinates of the independent oxide atoms and the first two Pd layers only, already a reasonable agreement between experiment and calculation was achieved, which is represented in the above-mentioned Pendry R factor of 0.45. Including buckling in the first Pd layer improved the agreement considerably to $R_{\mathrm{Pe}}=0.35$. After a determination of reasonable vibrational amplitudes for the oxide atoms, buckling of the oxide and of the first two Pd layers was optimized independently in several iterations resulting in an R_{Pe} of 0.27, strongly supporting the proposed model. Accordingly, the total number of free geometrical parameters in this analysis amounted to 18. An optimization of the vibrational amplitudes of the bulk atoms and the imaginary part of the inner potential was not performed for this structure due to time reasons and because the corresponding values gained from the analysis of the (2×2) structure were considered to be sufficiently applicable. Also an optimization of the in-plane coordinates of the oxygen atoms was omitted due to LEED's low sensitivity to these parameters at normal incidence and in order to prevent an unnecessary increase in the already rather high number of independent parameters. A comparison of all calculated I-V curves, using the best-fit structure, with the measured ones is presented in Fig. 6, showing satisfactory agreement for every single beam. Although the confirmation of the structure found by DFT is a convincing one ($R_{\mathrm{Pe}}=0.27$), we have to mention the fact that it is not possible to rule out all other potential candidates with LEED, since the total number of thinkable models is simply too large and the computational effort for every single model is extremely high. However, due to the very good agreement of every single coordinate of every oxide atom between the DFT and the LEED result (Table II), we regard the DFT model as unambiguously confirmed and hence the structure as solved.

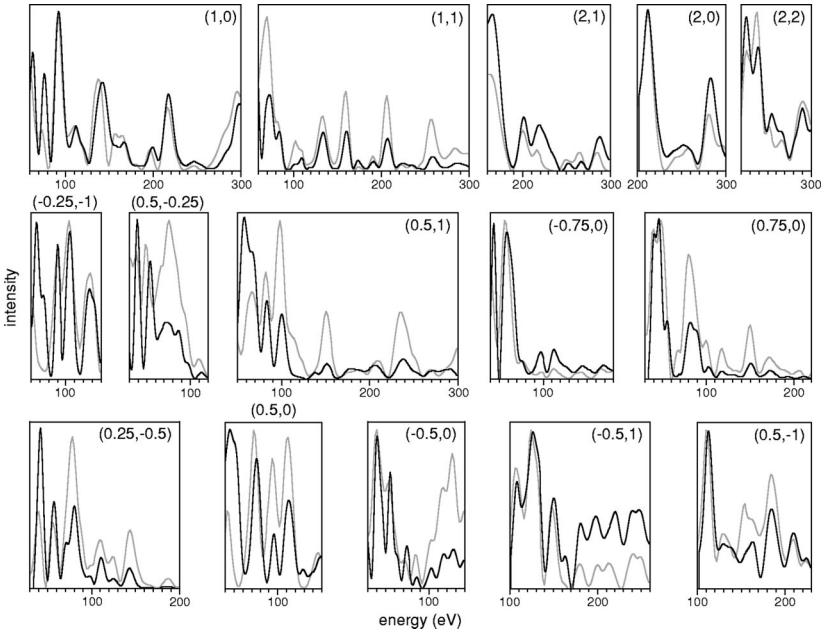

FIG. 6. Comparison between experimental (black) and calculated (gray) LEED I-V spectra of the best-fit model of the (4×4)-V_5O_{14} structure ($R_{Pe}=0.27$).

TABLE II. Comparison between LEED and DFT results concerning the geometry of the (4×4)-V_5O_{14} structure. Here, z denotes the height of an atom with respect to the center of gravity of the first Pd layer. Interlayer distances d_{ij} refer to the centers of gravity of the layers. DFT coordinates are scaled to the experimental lattice constant.

	LEED				**VASP**		
Atom	x (Å)	y (Å)	z (Å)	vib (Å)	x (Å)	y (Å)	z (Å)
O1	2.32	4.01	4.04 ± 0.18	0.28	2.32	4.05	4.16
O2	2.32	6.99	4.04 ± 0.18	0.28	2.34	6.96	4.15
O3	4.90	5.50	4.04 ± 0.18	0.28	4.85	5.48	4.16
O4	0.82	1.43	3.73 ± 0.18	0.22	0.84	1.45	3.79
O5	0.82	9.58	3.73 ± 0.18	0.22	0.84	9.54	3.75
O6	7.88	5.50	3.73 ± 0.18	0.22	7.85	5.48	3.77
V1	3.18	5.50	3.62 ± 0.05	0.17	3.18	5.50	3.66
V2	0.00	0.00	3.23 ± 0.07	0.18	0.00	0.00	3.29
V3	1.60	2.76	2.95 ± 0.03	0.20	1.66	2.84	2.99
V4	1.60	8.24	2.95 ± 0.03	0.20	1.66	8.14	2.98
V5	6.34	5.50	2.95 ± 0.03	0.20	6.22	5.47	3.00
O7	3.18	5.50	1.87 ± 0.30	0.20	3.18	5.48	2.04
O8	0.58	3.69	1.95 ± 0.10	0.24	0.58	3.62	2.02
O9	0.58	7.32	1.95 ± 0.10	0.24	0.58	7.33	2.01
O10	2.90	2.34	1.95 ± 0.10	0.24	2.92	2.29	2.06
O11	6.05	6.85	1.95 ± 0.10	0.24	6.07	6.80	2.02
O12	2.90	8.66	1.95 ± 0.10	0.24	2.91	8.67	2.02
O13	6.05	4.16	1.95 ± 0.10	0.24	6.06	4.11	2.05
O14	0.00	0.00	1.57 ± 0.30	0.20	0.02	0.00	1.64
O15					6.38	10.91	1.08
Pd1-6			0.04 ± 0.06	0.14			0.04
Pd7			0.04 ± 0.25	0.14			-0.02
Pd8-10			0.01 ± 0.07	0.14			0.04
Pd11-13			-0.01 ± 0.05	0.14			-0.05
Pd14-16			-0.11 ± 0.07	0.14			-0.05
Δd_{Pd12}			$+0.02\pm0.12$ (Å) (+0.9%)				-0.01 (Å) (-0.2%)
Δd_{Pd23}			-0.00 ± 0.14 (Å) (-0%)				0.00 (Å) (0.0%)
d_{bulk}			2.246 (Å)				2.246 (Å)

Finally, since this oxide has a very open structure, it is very likely that the above described preparation resulted in additional oxygen adsorbed in the center of the rings. This additional oxygen, which is not a part of the oxide, is depicted in Fig. 5 and labeled O15. However, it is not possible to verify the existence of this atom with LEED, since a correct treatment of the O15 atom would require the computation of a composite layer consisting of the oxide and the first Pd layer, which would involve an extremely high computational effort. More detailed information on the ''pocket-content,'' however, is given below. The coordinates of the best-fit structure obtained by LEED and the corresponding DFT values are given in Table II.

Further confirmation of the proposed structure is given by the comparison between measured and simulated STM images, where the latter ones were calculated based on the Tersoff-Hamann approximation[20] (Fig. 7). The interpretation of those images is very straightforward if one compares them with the structural model. The bright spots shown in the STM images are the vanadium atoms, where the brightness corresponds directly to their height. In that respect the brightest spots represent the V1 atoms of Fig. 5, the slightly darker ones the V2 atoms. In both cases, an oxygen atom is located between the vanadium atom and the palladium surface lifting the metal atom up considerably. The height difference of 0.4 Å is caused by the different adsorption sites of the oxygen atoms, which are on top for V1 and in the threefold hollow for V2. The lowest vanadium atoms V3, V4, and V5 are symmetry equivalent and can be seen as gray connections between the corners of the hexagons. The oxygen atoms, however, are not visible in the STM images.

3. Pocket content

As pointed out in the last paragraph, the content of the oxide pockets cannot be determined by LEED. DFT calcula-

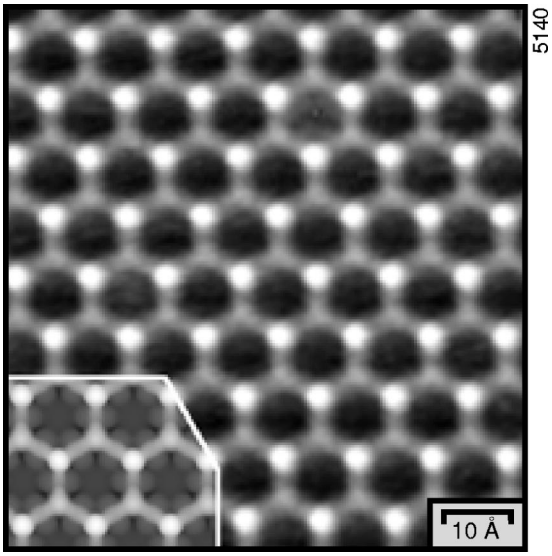

FIG. 7. Comparison of an experimental STM image of the (4×4) vanadium surface oxide structure (77×80 Å^2, −1 V, 0.46 nA, 0.3 ML) with a simulated image (inset in the bottom left corner).

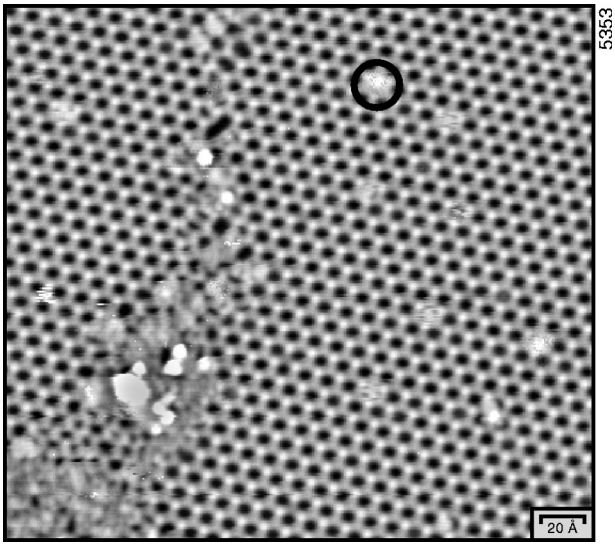

FIG. 8. STM image taken after the deposition of 0.2 ML Pd on the vanadium surface oxide (276×250 Å^2, −0.98 V, I=0.46 nA). The black circle marks one of the (4×4) hexagons, where a Pd atom was able to adsorb.

tions and physical reasoning, however, suggest an occupation with one oxygen atom. Further support for this point of view comes from STM images of the (4×4) structure after an additional deposition of 0.2 ML palladium. As shown in Fig. 8, the Pd atoms tend to agglomerate on the areas covered by the low-coverage phases, obviously due to the larger pocket space, whereas nearly no change of the (4×4) regions is observable. Taking a closer look reveals the fact that indeed some of the (4×4) pockets are filled, indicating former empty pockets. Arguing this way one finds that 97% of all pockets are occupied by an oxygen atom, preventing palladium adsorption. Keeping that in mind while taking a closer look at Fig. 7, one can indeed identify one single hexagon in the middle of the second row of the experimental STM image, which shows a nearly perfect agreement with the simulated one (calculated for an empty pocket), thus providing further evidence for the correctness of the presented analysis. The difference between simulated images with and without O in the pockets, however, is not sufficiently pronounced to unambiguously answer that question.

V. SUMMARY

The growth of very low coverages (<0.31 ML) of vanadium oxide on Pd(111), prepared by reactive evaporation, has been investigated by STM. At the lowest coverages, the formation of a nonperiodic structure composed of large hexagons (diameter ⩽22.1 Å) was observed, which partly started to transform into a quasiordered phase, consisting of (11×11) supercells, at about 0.15 ML. At a vanadium coverage of 0.2 ML an ordered (4×4)-V_5O_{14} oxide phase begins to develop, which eventually covers the entire surface (0.31 ML). Additionally, the total decomposition of the above described phases due to a reduction caused by the presence of hydrogen was investigated. Already after the exposure to 2.1 L of H_2 at room temperature the whole surface changed, showing a network of branches with local (2×2) symmetry. This structure, however, can be healed by annealing at 300 °C, resulting in a well-ordered (2×2)-V_2O_3 structure (not shown in this paper). Here, the same (2×2) phase was prepared by a hydrogen treatment at 300 °C immediately after the oxide formation. The well-ordered (2×2) and (4×4) structures have been analyzed by DFT and quantitative LEED, resulting in a confirmation of the models resulting from DFT studies by LEED.

The important result of the present study, however, is that tetrahedrally coordinated VO_4 units are stabilized on the Pd(111) surface in the low-coverage, oxygen rich limit. This is insofar intriguing as most bulk vanadium oxides exhibit an octahedral (or pyramidal) coordination. The substrate surface, therefore, makes a difference for thin oxides; it is capable to alter the preferential coordination of vanadium, although the vanadium atoms are not in direct contact to the substrate. The main reason for this behavior is that tetrahedral building units can be assembled into 1D chainlike structures, whereas octahedral units require a rather dense packing into 2D or 3D networks. The resulting 1D and open 2D structures facilitate an efficient coordination of oxygen atoms to the surface as well. The building units determined for the (4×4)-V_5O_{14} phase also serve as template for understanding the structures observed at even lower V coverages. It is possible to form 1D chains by interconnecting unit *E* of Fig. 4(f). We believe that chains with the sequence *D*-*E*-*E*-*D* are in fact corresponding to the edges of the larger hexagons observed at a coverage below 0.2 ML V. Unfortunately *ab initio* calculations for such large systems are presently out of reach.

Generally, the possibility to stabilize open unconventionally coordinated and reactive structures at metal surfaces

seems to be an interesting field of research. What catalytic properties does this network possess, and do such tetrahedral VO_4 units play a role for the catalytic properties of vanadium oxides? Further work will be required to elucidate these points.

ACKNOWLEDGMENTS

This work was sponsored by the Joint Research Program ''Gas-Surface Interactions'' of the Austrian *Fonds zur Förderung der wissenschaftlichen Forschung.*

[1] C.E. Julien, Mater. Sci. Eng., R. **40**, 407 (2003).
[2] R. Rella, P. Siciliano, A. Cricenti, R. Generosi, M. Girasole, L. Vanzetti, M. Anderle, and C. Coluzza, Thin Solid Films **349**, 254 (1999).
[3] G. Centi, Appl. Catal., A **147**, 267 (1996).
[4] S. Surnev, G. Kresse, M. Sock, M.G. Ramsey, and F.P. Netzer, Surf. Sci. **495**, 91 (2001).
[5] S. Chambers, Surf. Sci. Rep. **39**, 105 (2000).
[6] S. Surnev, G. Kresse, M.G. Ramsey, and F.P. Netzer, Phys. Rev. Lett. **87**, 86102 (2001).
[7] S. Surnev, L. Vitali, M.G. Ramsey, F.P. Netzer, G. Kresse, and J. Hafner, Phys. Rev. B **61**, 13 945 (2000).
[8] G. Kresse, S. Surnev, M.G. Ramsey, and F.P. Netzer, Surf. Sci. **492**, 329 (2001).
[9] S. Surnev, J. Schoiswohl, G. Kresse, M.G. Ramsey, and F.P. Netzer, Phys. Rev. Lett. **89**, 246101 (2002).
[10] S. Surnev, M. Sock, G. Kresse, J. N. Andersen, M. G. Ramsey, and F. P. Netzer, J. Phys. Chem. B **107**, 4777 (2003).
[11] R. Koller, W. Bergermyer, G. Kresse, C. Konvicka, M. Schmid, J. Redinger, R. Podloucky, and P. Varga, Surf. Sci. **512**, 16 (2002).
[12] V. Blum and K. Heinz, Comput. Phys. Commun. **134**, 392 (2001).
[13] J. Pendry, J. Phys. C **13**, 937 (1980).
[14] G. Kresse and J. Furthmüller, Phys. Rev. B **54**, 11 169 (1996).
[15] G. Kresse and D. Joubert, Phys. Rev. B **59**, 1758 (1999).
[16] E. Platzgummer, M. Sporn, R. Koller, M. Schmid, W. Hofer, and P. Varga, Surf. Sci. **453**, 214 (2000).
[17] C.I. Carlisle, T. Fujimoto, W.S. Sim, and D.A. King, Surf. Sci. **470**, 15 (2000).
[18] A. Michaelides, M.-L. Bocquet, P. Sautet, A. Alavi, and D.A. King, Chem. Phys. Lett. **367**, 344 (2003).
[19] G. Kresse, W. Bergermayer, R. Podloucky, E. Lundgren, R. Koller, M. Schmid, and P. Varga, Appl. Phys. A: Mater. Sci. Process. **A76**, 701 (2003).
[20] J. Tersoff and D.R. Hamann, Phys. Rev. B **31**, 805 (1985).